Experimental Flow Results in a Non-circular Duct with Heat Transfer Augmenting Obstacles

Azize Akcayoglu[1], Besir Sahin[2], Cetin Canpolat[3], and Huseyin Akilli[4]

***Abstract*—Present experimental study aims to examine flow differences generated by common flow up (CFU) and common flow down (CFD) vortex generator (VG) pairs fixed to the slant surfaces of an equilateral triangular duct. The flow differences were examined in detail in terms of formation of second set of twin vortices under different Reynolds number and duct conditions. It is concluded that the formation of twin vortices occurs an earlier downwind distance regardless of the value of Reynolds number and as the Reynolds number is increased from 3000 to 8000 the twin vortices disappear earlier in the case of CFD comparing to the case of CFU.**

***Index Terms*—PIV, Triangular duct, Vortex generator.**

I. INTRODUCTION

Heat transfer augmenting obstacles, including fins, ribs, wings, etc., fixed to the heat transfer enhancement surfaces are generally used for effectively cooling or heating of thermal systems, such as gas turbines, heat exchangers, electronics devices, and so on. In these applications, among other ducts, equilateral triangular ducts are preferred because of their superior heat transfer performance [1]–[4], lower fabrication costs [5], easy construction and higher mechanical strength [6]. The obstacles used in modern thermal systems destabilize the flow field, create swirl or vortices, and generate secondary flow field which are all responsible from enhancement of heat transfer. Among different types of obstacles, the triangular delta wing type VGs are more efficient [7], in terms of compactness criterion [8] and disturb continuously the viscous sub-layer [9] leading to a 3-D flow [10]. A comprehensive literature review on the subject was given by [11], [12].

In the literature according to some investigators [13], [14] heat transfer enhancement becomes better when a CFU configuration is used. Whereas some investigators [15]–[17] obtained higher heat transfer performance when a CFD configuration is used. Therefore in this experimental study it is aimed to help understanding of these discrepancies arised in the literature and hence to give more insight into the topic.

II. TEST MODELS AND EXPERIMENTS

In the present experiments two test ducts having the same dimensions, but with different VG orientations were used to study the flow differences generated by them. The total length of the equilateral triangular ducts was 69*D*, where *D* is the hydraulic diameter of the duct (Fig. 1). Two rows of delta wing type VGs were used for both ducts. In the first duct, the first and the second row of VGs were arranged in CFU orientation in which the distance between the leading edges of the VG pairs is greater than that of the trailing edges, whereas in the second duct the first row of VG pair was arranged in CFU and the second row was arranged in CFD orientation in which the distance mentioned above is smaller in that case (Fig. 2). Both the ducts and the VGs were made from 3-mm thick Plexiglass.

The leading edges of the VGs were placed 48*D* from the duct inlet. The axial distance between the trailing edges of the first row of VGs and the leading edges of the second row of VGs was 0.77*D*. Having a right triangle in shape, each VG had a horizontal and a vertical length of 0.77*D* and 0.22*D*, respectively. The angle of attack, defined as the angle between the flow direction and the centerline of the vortex generators, was 30°.

The present study was performed in a closed loop water channel having a settling chamber, a honey comb section and a 2-to-1 channel contraction section located at the inlet of the channel. The water was driven by a 15 kW centrifugal pump. Dantec Dynamics Flow Manager software and PIV system were used to measure the instantaneous velocity vector field. The velocity of the seeding particles made from silver-coated hollow glass spheres illuminated by using a double-pulsed Nd:YAG laser was recorded using a CCD camera with a

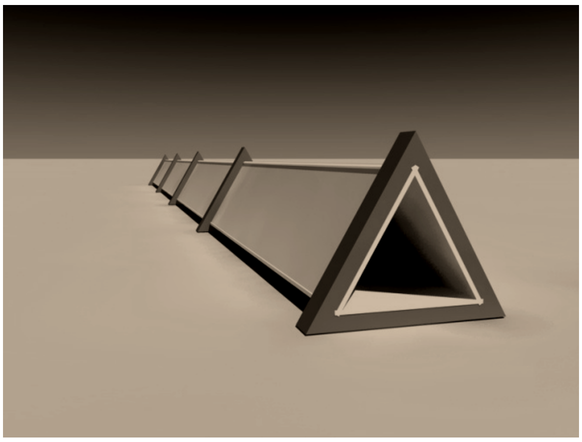

Manuscript received January 19, 2010. This work was supported by the Mechanical Engineering Department of Cukurova University under project no:AAP20025.

[1]A. Akcayoglu is with the Mersin University, Faculty of Technology, Mechanical Engineering Technology, Tarsus, Mersin, Turkey (corresponding author, phone: 324-627-4804; fax: 324-627-4805; e-mail: azize.akcayoglu@gmail.com).

[2]B. Sahin is with the Cukurova University, Faculty of Engineering and Architecture , Mechanical Engineering Department, Balcali, Adana, Turkey (e-mail: bsahin@cu.edu.tr).

[3]C. Canpolat is with the Cukurova University, Faculty of Engineering and Architecture , Mechanical Engineering Department, Balcali, Adana, Turkey (e-mail: cettincan@gmail.com).

[4]H. Akilli is with the Cukurova University, Faculty of Engineering and Architecture , Mechanical Engineering Department, Balcali, Adana, Turkey (e-mail: hakilli@cu.edu.tr).

ISBN: 978-988-18210-7-2
ISSN: 2078-0958 (Print); ISSN: 2078-0966 (Online)

Fig. 1. Equilateral triangular duct

resolution of 1024x1024 pixels. A high speed digital frame grabber was installed between the camera and a computer to transfer the measured vector field to the computer. Raw velocity vector fields were obtained from displacement vectors using a frame to frame cross correlation technique. The interrogation window size was 32x32 pixels providing 99x73 vectors over the entire flow field. Other details of the experimental system can be found in [18]–[20].

III. RESULTS

As the two sets of VG pairs were placed on the slant surfaces of the triangular ducts and as both pairs are responsible from formation of the twin vortices, then it is expected to get increased heat and momentum transfer characteristics where the twin vortices are formed. The flow measurements were performed at different locations inside the triangular ducts in order to specify the formation and disappearance distances of the twin vortices.

Fig. 3 indicates time-averaged vorticity contour plots obtained for the first duct at different downwind distances (x/*D*) where the twin vortices are appeared and disappeared. The minimum and incremental values of vorticity are $\omega_{min}=\pm 4\ s^{-1}$ and $\Delta x = 0.5\ s^{-1}$, respectively. Positive and negative vorticity are represented as solid and dashed lines, respectively. We observed that the twin vortices first appeared at x/*D*=50.88, 52.42, and 52.42 for Re=8000, 5000, and 3000 respectively (Figs. 3a,c,e). In addition, they disappeared at x/*D*=58.60, 58.60, and 61.68 for Re=8000, 5000, and 3000 respectively (Figs. 3b,d,f). We also noted that, the twin vortices are about to disappear at x/*D*=58.60 for Re=8000, and they are completely disappeared at x/*D*=58.60 and x/*D*=61.68 for Re=5000 and 3000, respectively, as shown in Figs. 3b,d,f.

Fig. 4 presents time averaged vorticity contour plot obtained for the second duct. The minimum and incremental values of vorticity are $\omega_{min}=\pm 3\ s^{-1}$ and $\Delta x = 0.5\ s^{-1}$, respectively. We noted that the twin vortices are first formed at x/*D*=49.77 regardless of the value of Reynolds number (Figs. 4a,c,e). They are disappeared at different downwind distances as shown in Figs. 4b,d,f. Kidney shaped vortices are observed for the second duct. This is due to the second row (CFD) of VG pairs of the second duct is oriented differently from the first row (CFU), as indicated in Fig. 2. Moreover, the vortex centers are found to be located closer to the side

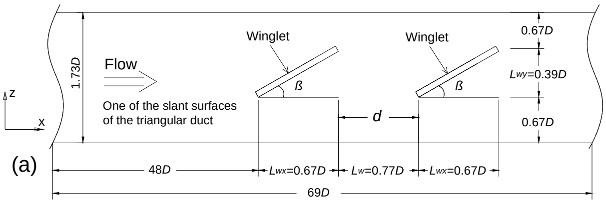

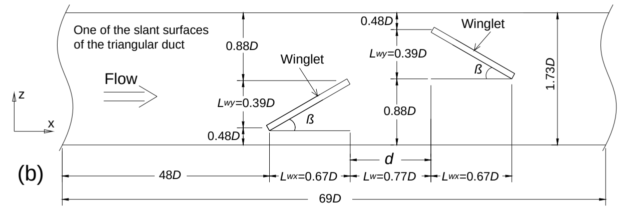

Fig. 2. Vortex generators mounted on the slant surfaces of the ducts. (a) First duct, (b) Second duct

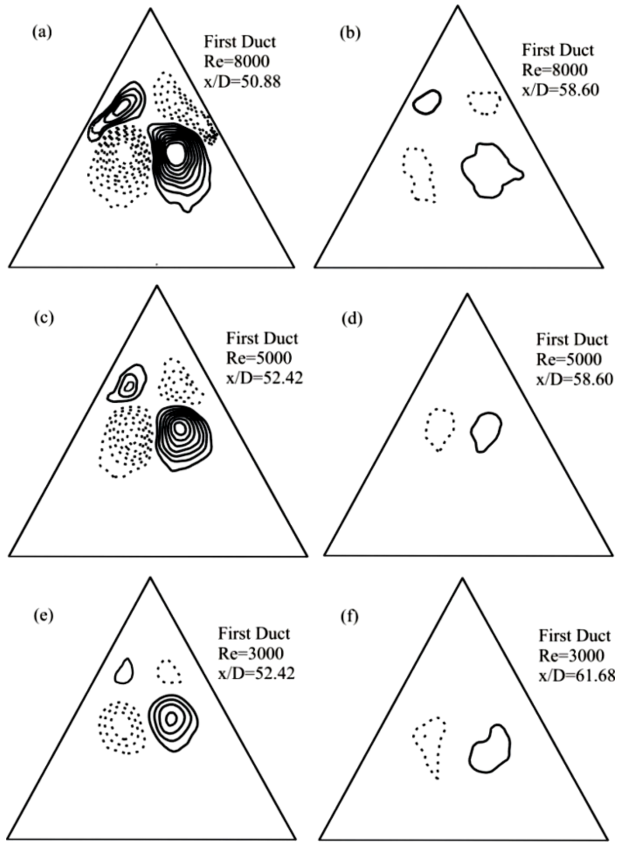

Fig. 3. Time-averaged vorticity contours obtained for the first duct.

walls of the second duct due to the fact that the VG pairs were fixed closer (0.48*D*) to the corners of the second duct compared with the first duct (0.67*D*), as shown in Fig. 2. Comparing Figs. 3 and 4 it is clearly seen that the twin vortices are formed and disappeared in an earlier downwind distance for the second duct, compared with the first duct. Another observation is that, for each Reynolds number, a larger area is observed below the lower twin vortices in the case of the second duct comparing to the case with the first duct, as illustrated in Figs. 3 and 4. In this area a downflow region occurs which is again an indication of higher heat transfer rate. It is also another interesting point to note that the centers of the lower and upper twin vortices are located closer to the apex of the triangular duct in the case of the second duct, comparing to case of the first duct. The vorticity pairs illustrated in Figs. 3 and 4 are not completely symmetric, because of the side wall effects of the ducts and of the fact that they just begin to form. Their shapes are completely symmetric at subsequent downwind distances just after the formation.

We plotted Fig. 5 in order to compare the shape, structure, and location of the centers of the twin vortices obtained for both ducts, for Re=5000 at x/*D*=50.88. A counter rotating vortex pair and a second set of vortex pair is observed for the first and the second duct, respectively. The vortex formation area is larger for the second duct, compared with the first duct. Induced vorticity field between the vortex pairs is found larger for the second duct, comparing to the first duct. Some weaker concentrations of vorticity near the base of the duct are observed only for the second duct. The induced vorticity field, which is observed only for the second duct, is also an indication of better heat transfer characteristics.

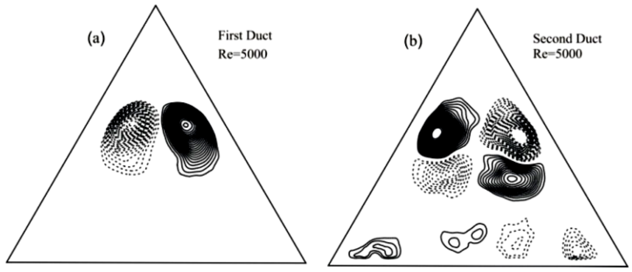

Fig. 5. Time-averaged vorticity contours obtained for the First and the Second Duct at x/*D*=50.88.

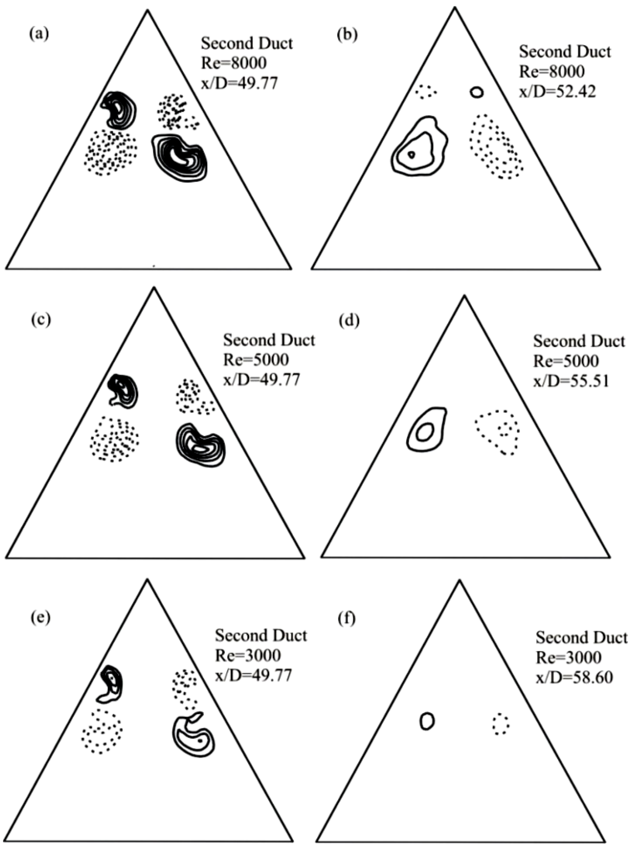

Fig. 4. Time-averaged vorticity contours obtained for the Second Duct.

IV. Conclusion

The distances of formation and disappearance of the second set of twin cortices is determined considering different Reynolds number and duct geometric conditions. As the Reynolds number is increased from 5000 to 8000, the second set of twin vortices is formed earlier and when it is increased from 3000 to 5000, the twin vortex formation location remains the same in the case of first duct. On the other hand, the second duct is able to form the second set of twin vortices at x/*D*=48.77 regardless of the value of Reynolds number. Therefore, for the second duct, it can be concluded that the formation of the second set of twin vortices is only affected by location and configuration of the VGs and is not affected by the value of Reynolds number between 3000-8000. In the second duct, the non-dimensional streamwise distance (x/*D)* for the formation of twin vortices increases as Reynolds number decreases. The second set of twin vortices is able to show its affect in the larger downwind distance in the first duct compared with the second duct for Re=8000, 5000, and 3000. The information obtained from present experiments can be used to find out where to locate the subsequent VG pairs in order to get increased heat transfer coefficients inside the ducts. For example, for the first duct, there is no need to insert any vortex generator pair between x/*D*=50.88 and x/*D*=58.60 for Re=8000 since the effect of the second set of twin vortices did not disappear in the specified locations of the duct. As another example, for the second duct, there is no need to insert any VG pair between x/*D*=49.77 and x/*D*=58.60 for Re=3000. As the induced flow field between the vortex pairs increases the heat transfer, and as the flow field between the vortex cores is found larger in the case of the second duct, therefore, it is expected to obtain better heat transfer characteristics for the second duct compared with the first duct.

References

[1] R. Gupta, P.E. Geyer, D.F. Fletcher, B.S. Haynes, “Thermohydraulic performance of a periodic trapezoidal channel with a triangular cross-section,” *Int, J. Heat Mass Transfer*, vol. 51, 2008, pp. 2925–2929.

[2] C.W. Leung, S.D. Probert, “Forced-convective turbulent flows through horizontal ducts with isosceles-triangular internal cross-sections,” *App. Energy*, vol. 57:1, 1997, pp. 13-24.

[3] R.K. Shah, A.L. London, *Laminar Flow Forced Convection in Ducts.* Academic Press, New York, 1978.

[4] L.Z. Zhang, “Comparison of heat transfer performance of tube bank fin with mounted vortex generators to tube bank fin with punched vortex generators,” *Exp. Thermal and Fluid Sci.*, vol. 33, 2008, pp. 58–66.

[5] S.W. Ahn, K.P. Son, “Heat transfer and pressure drop in the roughened equilateral triangular duct,” *Int. Comm. Heat Mass Transfer*, vol.29:4, 2002, pp. 479-488.

[6] L.Z. Zhang, “Laminar flow and heat transfer in plate-fin triangular ducts in thermally developing entry region,” *Int. J. Heat and Mass Transfer*, vol. 50, 2007, pp. 1637–1640.

[7] R. Vasudevan, V. Eswara, G. Biswas, “Winglet type vortex generators for plate fin heat exchangers using triangular fins,” *Numerical Heat Transfer, Part A*, vol. 58, 2000), pp. 533-555.

[8] P.M. Nakod, S.V. Prabhu, R.P. Vedula, “Heat transfer augmentation between impinging circular air jet and flat plate using finned surfaces and vortex generators,” *Experimental Thermal and Fluid Science*, vol. 32, 2008, pp. 1168–1187.

[9] F.P. Incropera D.P. DeWitt, *Introduction to Heat Transfer.* John Wiley & Sons, USA, 1996.

[10] S. Ferrouillat, P. Tochon, C. Garnier, H. Peerhossaini, “Intensification of heat-transfer and mixing in multifunctional heat exchangers by artificially generated streamwise vorticity,” *Applied Thermal Engineering*, vol. 26, 2006, pp. 1820–1829.

[11] Q. Wang, Q. Chena, L. Wang, M. Zenga, Y. Huangc, Z. Xiao, “Experimental study of heat transfer enhancement in narrow rectangular channel with longitudinal vortex generators,” *Nuclear Engineering and Design*, vol. 237, 2007, pp. 686–693.

ISBN: 978-988-18210-7-2
ISSN: 2078-0958 (Print); ISSN: 2078-0966 (Online)

[12] A.M. Jacobi, R.K. Shah, “Heat transfer surface enhancement through the use of longitudinal vortices:a review of recent progress,” *Exp. Thermal Fluid Sci*, vol. 11, 1995, pp. 295–309.
[13] K. Torii, K.M. Kwak, K. Nishino, “Heat transfer enhancement accompanying pressure-loss reduction with winglet-type vortex generators for fin-tube heat exchangers,” *Int. J. Heat and Mass Transfer*, vol. 45, 2002, pp. 3795–3801.
[14] C.B. Allison, B.B. Dally, “Effect of a delta-winglet vortex pair on the performance of a tube–fin heat exchanger,” *Int. J. Heat and Mass Transfer*, vol. 50, 2007, pp. 5065–5072.
[15] Kim, E., and Yang, J.S., “An experimental study of heat transfer characteristics of a pair of longitudinal vortices using color capturing technique,” *Int. J, Heat and Mass Transfer*, vol. 45, 2002, pp. 3349–3356.
[16] M. Fiebig, A.Valencia, N.K. Mitra, “Wing-type vortex generators for fin and tube heat exchangers,” *Exp. Thermal Fluid Sci*, vol. 7, 1993, pp. 287–295.
[17] G. Biswas N.K. Mitra, M. Fiebig, “Heat transfer enhancement in fin-tube exchangers by winglet type vortex generators,” *Int J Heat Mass Transfer*, vol. 37, 1994, pp. 283–291.
[18] N.A. Ozturk, A. Akkoca, B. Sahin, “PIV measurements of flow past a confined cylinder,” *Exp. in Fluids*, vol. 44, 2008, pp. 1001–1014.
[19] N.A. Ozturk, A. Akcayoglu, B. Sahin, “Downstream particle image velocimetry measurements of a circular cylinder-plate junction,” *Proc. Inst. Mech. Eng,. Part C: J. Mech. Eng. Sci.*, vol. 223(8), 2009, pp. 1837–1849.
[20] A. Akcayoglu, “Flow past confined delta wing type vortex generators,” *Exp. Thermal and Fluid Sci*, submitted for publication.

ISBN: 978-988-18210-7-2
ISSN: 2078-0958 (Print); ISSN: 2078-0966 (Online)